ICSV14
Cairns • Australia
9-12 July, 2007

14th International Congress on Sound & Vibration

THE DYNAMIC CHARACTERISTICS OF SMA HELICAL SPRING IN AXIAL VIBRATORY MOTION

Chun-Ying Lee, Chia-Wei Hsu

Department of Mechanical and Automation Engineering
Da-Yeh University, Changhua 515, Taiwan
leech@mail.dyu.edu.tw

Abstract

The helical spring is capable of providing the flexibility in more than one axis and the shape memory alloy (SMA) has the tuneable mechanical property controlled by the temperature change and stress, etc. Therefore, the use of SMA helical spring in the vibration platform with controllability in multi-directions could find application in the many aspects. For example, the suspension spring for an optical disk drive. In this study, the axial vibratory characteristics of the helical spring made of SMA are investigated. The shear strain of the SMA spring wire is assumed as a linear distribution and is proportional to the radius from the centre of the wire, when the spring is subjected to axial loading. However, the SMA undergoes phase transformation between martensite and austenite at different stress and temperature. Therefore, the mechanical behavior of the spring changes with respect to the amplitude of vibration and the controlled temperature. The constitutive relation of the SMA proposed by Brinson is adopted and the hysteresis loop due to the martensitic transformation is considered. An approach of equivalent strain energy is employed to derive the apparent stiffness of the spring in different vibratory amplitudes and temperatures, with the consideration of different Young's moduli for different phases. The energy enclosed by the hysteresis loop is accounted for the study of the damping capacity of the spring. The experimental setups for quasi-static deflection test and sprung-mass vibration test have been constructed, respectively. Both the simulated results and experimental measurements show the decrement in spring constant with respect to the deflection amplitude. In the meanwhile, the damping property increases with the raise in deflection amplitude. It is shown the formulation can be applied in the design of the SMA helical spring.

1. INTRODUCTION

The increasing demand for the high precision machinery with better performance has offered the engineers with challenges in suppression of vibration. Shape memory alloy (SMA), along with other smart materials, can change its material properties under the influence of control parameters. The state-switched systems designed with the incorporation of smart materials provide the capability for actively tuned vibration suppression [1].

Possible geometry application for the SMA in vibration control can be wire, disk and helical spring, etc. The Young's modulus of the SMA increases from martensite to austenite with the actuation of heat and/or strain. The composite beam with embedded SMA wires [2], vibration absorber in the form of cantilever SMA beam [3], and compression helical spring [4], etc. are some examples of employing the tunable property of the SMA in the literature. Among them, the form in helical spring offers the flexibility in multi-directions: axial, transverse, torsion and bending. Therefore, it has been proposed the use of SMA helical spring in the suspension platform of an optic disk drive [5].

In order to design a SMA component with the desired property, the constitutive relation must be formulated. Prahlad and Chopra reviewed and compared constitutive models for SMA behavior under uni-axial loading with experimental data over the entire thermomechanical range of test conditions [6]. In this study, the one dimensional constitutive model proposed by Brinson [7] was adopted due to its simplicity and capability of predicting both the shape memory effect and the superelastic behavior. For the purpose of formulating the equivalent spring constant and damping coefficient of a SMA helical spring, the strain energy and dissipated energy of the material under axial loading were calculated first. Then, the constitutive relation of the SMA in shear was incorporated into the formulation of the helical spring. Based on the equivalent maximum strain energy, the linearized spring constant of the helical spring under the same deformation amplitude can be derived. On the other hand, the ratio of the dissipated energy to the maximum strain energy gives rise to the damping coefficient of the spring.

2. THEORETICAL FORMULATION

The one dimensional constitutive model for SMA material under uniaxial loading proposed by Brinson [7] is adopted herein. For the SMA wire wound as helical spring and subjected to axial loading, the reactions over the cross-section consist of transverse shear and torsion loadings. Under the geometrical configuration usually used, the deformation contributed by the transverse shear can be neglected comparing to its torsional counterpart [8]. Hence, the SMA wire only under simple torsion loading is considered in this study. According to the axial displacement at the end of the helical spring is related to the torsional deformation of the wire, the linearized spring constant k can be formulated thru the equivalence in strain energy:

$$U = \frac{1}{2}k\delta^2 = \int_0^L \int_0^r 2\pi\rho u(\gamma) d\rho\, dL\,, \tag{1}$$

where $u(\gamma)$ is the strain energy density defined as the area below the stress-strain curve up to the shear strain γ. L is the length of the SMA wire which can be calculated as $L = 2\pi R N_A$. In the above equations, r and R denote the radii of the wire and coil, respectively, while ρ the radial coordinate from the centre of the wire. δ is the associate deflection of the spring at its end with the maximum shear strain in the wire reaching $\gamma_{\max}$, or

$$\gamma_{\max} = r\frac{\delta}{2\pi R^2 N_A}\,. \tag{2}$$

N_A represents the number of active coils of the spring. The state of the SMA can be determined by the temperature and the magnitude of the stress. It has been proposed by Brinson for the SMA material subjected to uniaxial loading. The constitutive equation for the SMA material under simple shear can be written as

$$\tau - \tau_0 = G(\xi)\gamma - G(\xi_0)\gamma_0 + \frac{\Omega(\xi)}{\sqrt{3}}\xi_s - \frac{\Omega(\xi_0)}{\sqrt{3}}\xi_{s0}\,, \tag{3}$$

where ξ and ξ_s are the total martensite fraction and stress-induced detwinned martensite fraction, respectively. Ω denotes the transformation constant related to the uniaxial normal loading. It should be noted that uniform temperature change would not induce the shear deformation. Therefore, the term associated to the thermal coefficient of expansion has been dropped comparing to its uniaxially loaded counterpart. Furthermore, the transformation constant Ω is defined as

$$\Omega(\xi) = -\varepsilon_L E(\xi)\,. \tag{4}$$

ε_L is the maximum residual strain for the SMA material. *E* and *G* are the elastic modulus and shear modulus those are related to each other by the relationship:

$$G = \frac{E}{2(1+\nu)} \tag{5}$$

Since the microstructure of the SMA material under the influence of temperature and stress may consist of martensite and austenite, the resulted elastic modulus is assumed to follow the rule of mixture, i.e.

$$G(\xi) = G_m\xi + G_A(1-\xi) \tag{6}$$

Since the stress-strain equation cannot be written explicitly in terms of strain function, the strain energy density is calculated by using trapezoidal rule of numerical integration. The thus obtained strain energy density is plugged into Eqn(1) and Gaussian quadrature method is employed to obtain the integration over the radius.

Because of the shape memory effect or the superelastic behaviour, the unloading process of the SMA wire might not follow the loading path in reverse direction. Hence, a hysteresis loop would form upon loading-unloading process. The dissipated energy ΔU enclosed by the hysteresis loop can be calculated similarly by accounting the unloading segment into Eqn(1). The damping coefficient of the SMA under this specific loading can be estimated as $\Delta U/U$.

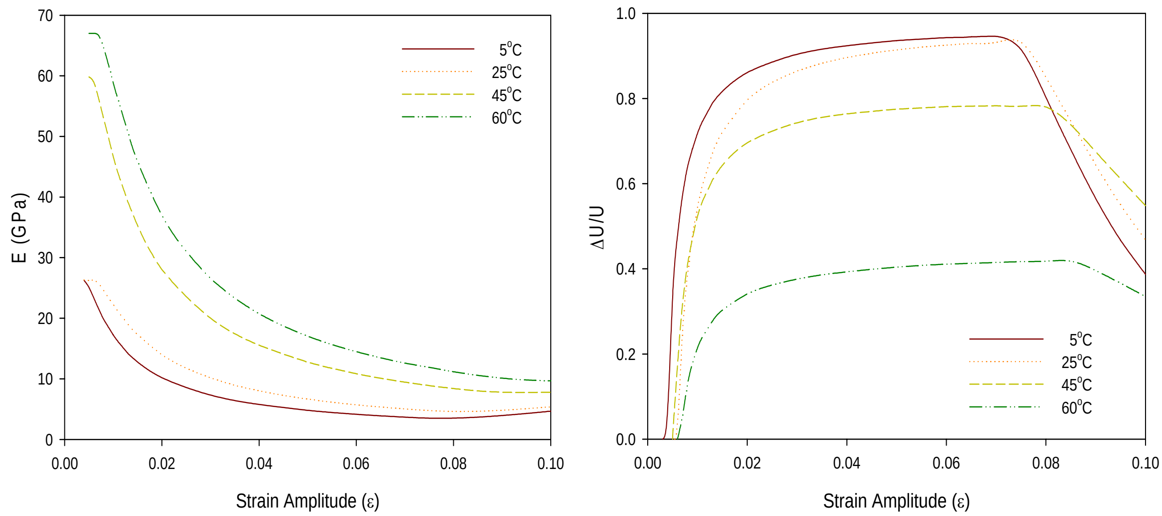

(a) (b)

Figure 1. The variation of: (a) the equivalent Young's modulus, (b) damping property of SMA with respect to strain amplitude under uni-axial loading at different temperatures.

By using the equivalent strain energy formulation in this study and adopting the material parameters of Brinson [7], Figure 1(a) demonstrates the variation of the equivalent Young's modulus of SMA with respect to strain amplitude under uniaxial loading at different temperatures. The equivalent Young's modulus decreases with the increasing amplitude of strain for all temperatures except for strain greater than the maximum residual strain 0.067 at martensitic phases. The decrement in the modulus is due to the induced strain from detwinning of the martensite while the increment to the hardening of the detwinned martensite. The associate change in damping coefficient is presented in Figure 1(b). On the contrary to those of equivalent Young's modulus, the damping coefficient increases first with the strain amplitude, and then drops as the maximum residual strain is exceeded. Moreover, the damping coefficient is larger in magnitude for the martensite than the austensite because of the shape memory effect.

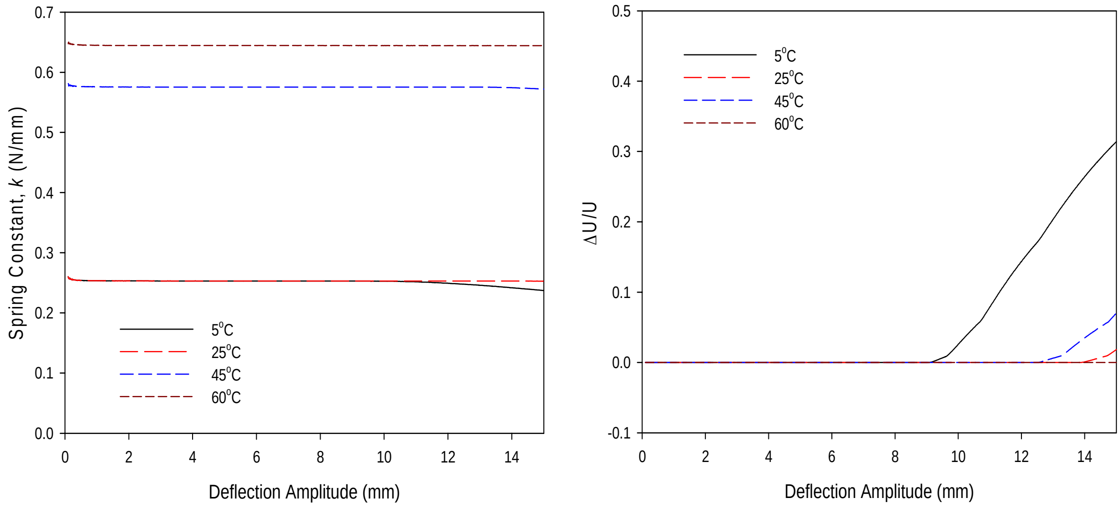

(a) (b)

Figure 2. The variation of: (a) the equivalent spring constant, (b) damping property, of a helical SMA spring with respect to displacement amplitude under longitudinal loading at different temperatures.

By considering the helical SMA spring in axial compression, the equivalent spring characteristics based on the former formulation are presented in Figure 2. Figure 2(a) shows the change in spring constant with respect to the amplitude of axial compression at four different temperatures. Basically, the spring constant does not decrease significantly as the deflection is raised. The slightly decrease in spring constant with deflection amplitude is due to the induced detwinning of the martensite at low temperatures. While at higher temperatures, the thermally induced martensite-to-austenite transformation renders the increment in austenite content. Consequently, the apparent spring constant becomes larger in magnitude because of the higher shear modulus for austenite phase comparing to the martensite. The associate variation of damping property in the simulated analysis is presented in Figure 2(b). Since only the dissipated energy accompanying the detwinning and phase transformation is considered herein and the hysteresis due to the martensite or the austenite alone is neglected, the damping coefficient at small deflection amplitude remains zero. The damping at 5^{o}C demonstrates the significant increment at larger deflection. It is because the shape memory effect of the martensite phase prevails under low temperature environment.

3. EXPERIMENTAL MEASUREMENT AND DISCUSSION

In order to understand the mechanical behaviour of the SMA wire used in this study, a static test setup for measuring the loading-deflection relation is established as shown schematically in Figure 3. The SMA spring used in this study was a commercial product distributed by Jameco Electronics. The mean diameter of the coil and the diameter of the wire are 7*mm* and 1*mm*, respectively. The number of active coils is 8.5. Due to the unavailability of the material property, an axial loading testing apparatus was set up to study the phase transformation characteristics of the SMA spring. Figure 3 shows the schematic diagram of the experimental setup. The SMA spring was loaded in between two Teflon insulating spacers. The insulating spacers confined the electric current only thru the spring to raise its temperature via ohmic effect. The control module controlled the current supply and the temperature was monitored by a thermocouple. As to the measurement of mechanical loading and the associate deflection, the deflection was imposed by adjusting the clamped length of the micrometer while the serial connected load cell kept track the corresponding compressive loading. The equivalent spring constant and damping property are obtained by the maximum strain energy U and the associate dissipated energy ΔU/U mentioned in the previous section.

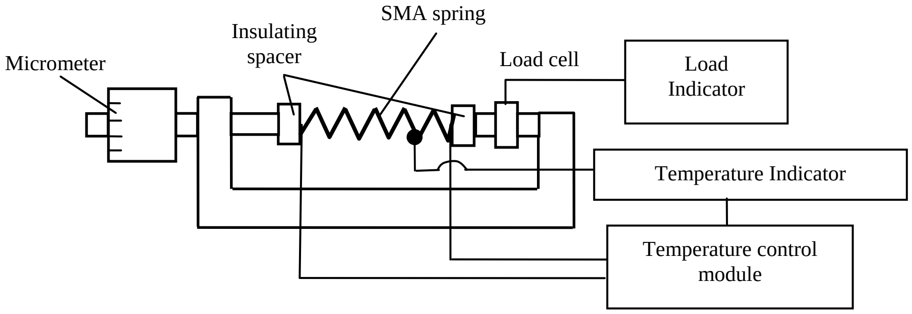

Figure 3. Schematic diagram of the apparatus for static test of axial loaded SMA spring

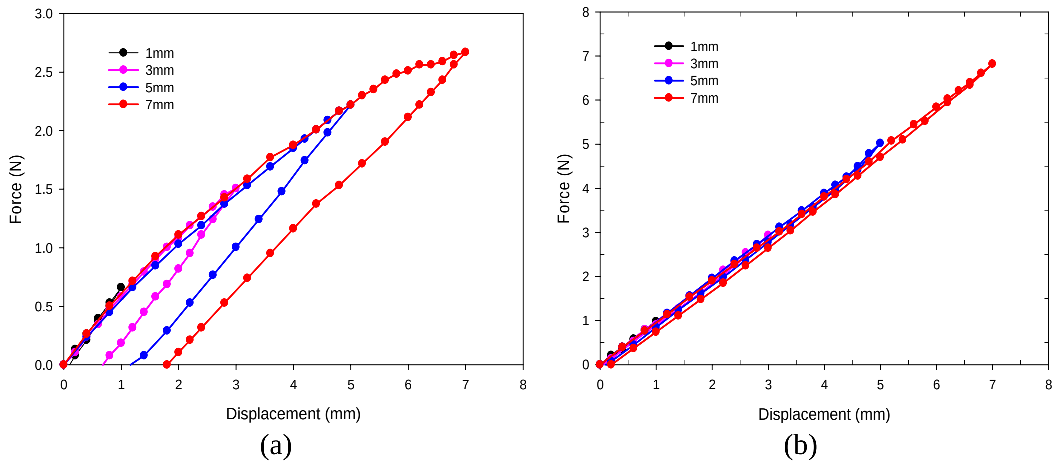

Figure 4. The measured loading-unloading loops of axially loaded SMA spring at different deflection amplitudes: (a) 25°C; (b) 80°C

Figure 4 presents the measured loading-unloading loops of the spring at four different deflection amplitudes and two temperatures. At room temperature (25°C), the spring showed obvious shape memory effect while nearly elastic at high temperature 80°C. The maximum deflection amplitude was limited to 7mm because the buckling occurred for larger deflection. It must be mentioned that at 25°C, the spring was observed to have stress relaxation. In other words, the reading from the load cell took a period of time to settle to a steady value after the instant the deflection was adjust to the next step. Therefore, the calculated spring constant and damping property presented in Figure 5 are labelled as unrelaxed and relaxed ones. The results clearly demonstrate that the spring constant decreases with the increasing deflection amplitude while the damping property in the opposite trend. The relaxed results due to the slight diminishing loading at the same deflection give smaller spring constant and larger damping. The discrepancy between the relaxed and unrelaxed results is widened as the deflection amplitude increases. At 80°C, the SMA transforms from martensite to austenite, the spring demonstrates higher stiffness and less sensitive to the deflection amplitude. The superelastic property was not observed in these measurements because of the limited imposition in the deflection.

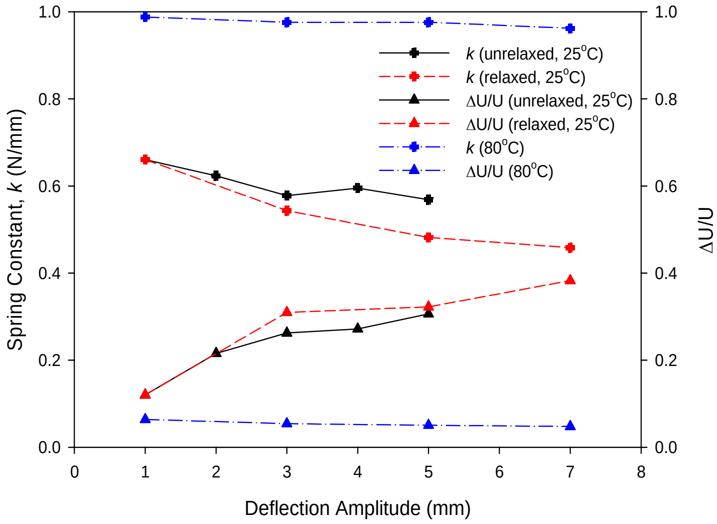

Figure 5. The calculated spring characteristics based on the measured loading-unloading loops presented in Figure 4.

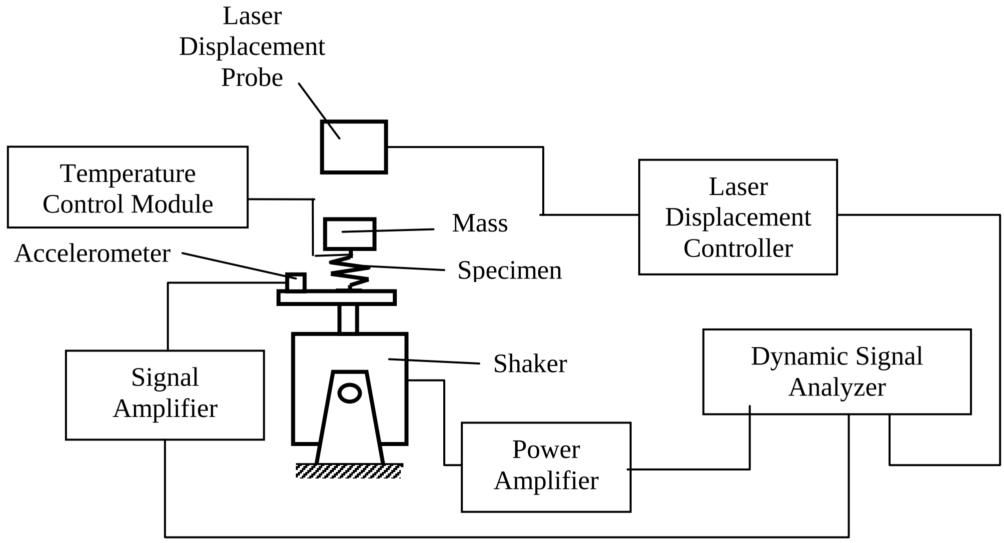

Figure 6. The schematic diagram of the test apparatus for dynamic measurement of SMA spring-mass system in longitudinal vibration

The dynamic characteristics of the SMA spring in longitudinal vibration were investigated using the experimental setup shown schematically in Figure 6. The spring-mass system was excited in base vibration by a mechanical shaker. The excitation was measured by the accelerometer mounted on the base while the resulted vibration displacement of the mass was detected by the laser displacement probe. The measurement was performed by employing swept-sine technique. Both the mass displacement and the base vibration were processed by the dynamic signal analyzer to find the resonance frequency of the system. The associated spring constant was then found by using the relationship between the measured resonance frequency and the sprung mass: $k = m\omega^2$. The temperature of the spring was controlled by the heating compartment encasing the system. The SMA spring used was the same as the static test except the number of active coils was reduced to 5.

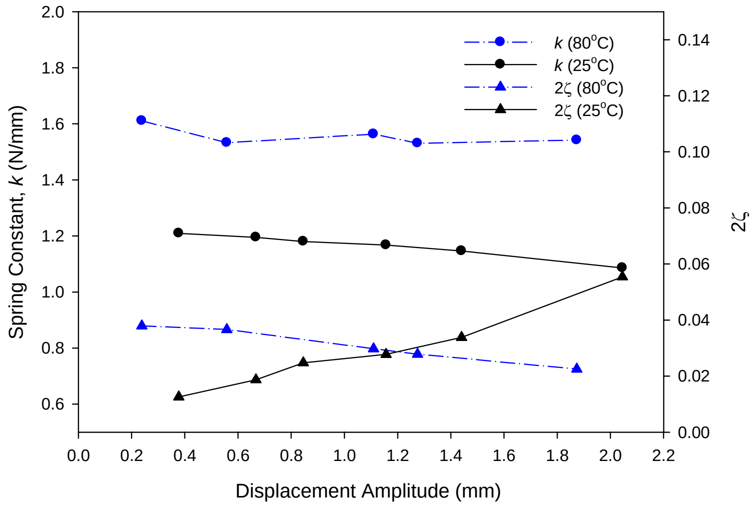

Figure 7. The characteristics of the SMA spring with respect to vibratory amplitude measured by swept-sine technique at two different temperatures.

Figure 7 presents the dynamic characteristics of the SMA spring with respect to the displacement amplitude at two different temperatures: 25^{o}C and 80^{o}C. It shows that the spring constant decreases with the increment of vibratory amplitude at low temperature which the SMA is in martensite. However, at high temperature when the SMA is in austenite, the spring constant remains less influenced by the vibratory amplitude. These results, as well as the results in Figure 6, are in consistent trend with the simulated ones in Figure 2. The variation of the damping property with respect to the vibratory amplitude, on the other hands, shows increasing and decreasing trends for SMA at 25^{o}C and 80^{o}C, respectively. They are also consistent with the quasi-static measurements presented in Figure 6. The higher level of the damping measured at 80^{o}C for the vibratory testing comparing to its quasi-static counterpart could be caused by the heating wire connection.

4. CONCLUSIONS

The spring constant and damping property of a SMA helical spring have been formulated by incorporating the constitutive model proposed by Brinson. The strain energy and the dissipated energy of the loading-unloading loop for the spring under axial deflection were employed to obtain the linearized spring characteristics. With the simulated results of the SMA wire under axial loading, it was found that the equivalent Young's modulus decreases with the increment of strain amplitude after the initial linear elastic range. The damping property, on the other hand, increases firstly with the strain amplitude while it decreases after the maximum residual strain is exceeded. The adoption of the formulation in helical spring shows that slight decrement in spring constant with the deflection amplitude within the deflection range studied. The flexibility provided by the helical configuration renders the difficulty in rasing the magnitude of the torsional shear strain. Therefore, the significant decrement in spring constant was not seen the simulated result. Similarly, the drop in damping property was not reached.

The experimental measurements for both quasi-static deflection and sprung-mass vibration test have shown the similar trends of the influence of deflection amplitude on the spring characteristics comparing to the simulated results. However, because of the unavailability in the material constants of the used SMA metal, the quantitative verification of the formulation proposed in this study is not performed. In addition, the stress relaxation of the SMA spring under axial loading was observed. These viscoelastic characteristics can be the subject for the modelling of further study.

ACKNOWLEDGEMENT

The financial support from National Science Counsel, Taiwan, under Grant No. NSC 95-2221-E-212-004-MY3 is gratefully acknowledged.

REFERENCES

[1] K.A. Cunefare, S. DeRosa, N. Sadegh and G. Larson, “State-Switched Absorber for Semi-Active Structural Control,” *Journal of Intelligent Material Systems and Structures* 11, 300-310 (2000).

[2] Wong, W. H., Tse, P. C., Lau, K. J., Ng, Y. F., “Spring Constant of Fibre-reinforced Plastics Circular Springs Embedded with Nickel-Titanium Alloy Wire,” *Composite Structures*, **65**, 319-328 (2004).

[3] Williams, K., Chiu, G. and Bernhard, R., “Adaptive-Passive Absorbers Using Shape-Memory Alloys,” *Journal of Sound and Vibration*, **249**, 835-848 (2002).

[4] Liang, C. Rogers, C. A., “Design of Shape Memory Alloy Springs with Applications in Vibration Control,” *Journal of Vibration and Acoustics*, **115**, 129-135 (1993).

[5] C.Y. Lee, C.S. Lin and H.C. Zhao, “Dynamic Characteristics of Platform with SMA Helical Spring Suspension,” *Proceedings of the Thirteenth International Congress on Sound and Vibration* (ICSV13), 2-6 July 2006, Vienna, Austria.

[6] H. Prahlad and I. Chopra, “Comparative Evaluation of Shape Memory Alloy Constitutive Models with Experimental Data,” *Journal of Intelligent Material Systems and Structures* 12, 383-395 (2001).

[7] L.C. Brinson, “One-Dimensional Constitutive Behavior of Shape Memory Alloys: Thermomechanical Derivation with Non-Constant Material Functions and Redefined Martensite Internal Variable,” *Journal of Intelligent Material Systems and Structures* 4, 229-242 (1993).

[8] J.E. Shigley, C.R. Mischke, and R.G. Budynas, *Essentials of Mechanical Engineering Design*, McGraw-Hill Co., Singapore, 2004.